

# A coherence parameter characterizing generative compressed sensing with Fourier measurements

Aaron Berk, Simone Brugiapaglia, Babhru Joshi, Yaniv Plan, Matthew Scott and Özgür Yilmaz

**Abstract**—In [Bora et al. \(2017\)](#), a mathematical framework was developed for compressed sensing guarantees in the setting where the measurement matrix is Gaussian and the signal structure is the range of a generative neural network (GNN). The problem of compressed sensing with GNNs has since been extensively analyzed when the measurement matrix and/or network weights follow a subgaussian distribution. We move beyond the subgaussian assumption, to measurement matrices that are derived by sampling uniformly at random rows of a unitary matrix (including subsampled Fourier measurements as a special case). Specifically, we prove the first known restricted isometry guarantee for generative compressed sensing with *subsampled isometries*, and provide recovery bounds with nearly order-optimal sample complexity, addressing an open problem of [Scarlett et al. \(2022, p. 10\)](#). Recovery efficacy is characterized by the *coherence*, a new parameter, which measures the interplay between the range of the network and the measurement matrix. Our approach relies on subspace counting arguments and ideas central to high-dimensional probability. Furthermore, we propose a regularization strategy for training GNNs to have favourable coherence with the measurement operator. We provide compelling numerical simulations that support this regularized training strategy: our strategy yields low coherence networks that require fewer measurements for signal recovery. This, together with our theoretical results, supports coherence as a natural quantity for characterizing generative compressed sensing with subsampled isometries.

**Index Terms**—Generative neural network, subsampled isometry, compressed sensing, coherence, Fourier measurements

## I. INTRODUCTION

The solution of undetermined linear inverse problems has many important applications including geophysics ([Herrmann et al., 2012](#); [Kumar et al., 2015](#)) and medical imaging ([Adcock and Hansen, 2021](#); [Lustig et al., 2008](#)). In particular, compressed sensing permits stable and robust order-optimal recovery of signals that are well represented by one of a certain set of structural proxies (e.g., sparsity) ([Foucart and](#)

This manuscript was submitted 19 July, 2022. A. Berk is partially supported by Institut de valorisation des données (IVADO) and Centre de recherches en mathématiques (CRM) Applied Math Lab. S. Brugiapaglia is partially supported by NSERC grant RGPIN-2020-06766 and the Faculty of Arts and Science of Concordia University. B. Joshi is supported in part by the Pacific Institute for the Mathematical Sciences (PIMS). Y. Plan is partially supported by an NSERC Discovery Grant (GR009284), an NSERC Discovery Accelerator Supplement (GR007657), and a Tier II Canada Research Chair in Data Science (GR009243). Ö. Yilmaz is supported in part by an NSERC Discovery Grant (22R82411), and a UBC Data Science Institute grant.

A. Berk is with McGill University, Montréal, QC, Canada (aaron.berk@mcgill.ca)

S. Brugiapaglia is with Concordia University, Montréal, QC, Canada (simone.brugiapaglia@concordia.ca)

B. Joshi, Y. Plan, M. Scott & Ö. Yilmaz are with the University of British Columbia, Vancouver, BC, Canada ({b.joshi, yaniv, matthewscott, oyilmaz}@math.ubc.ca)

[Rauhut, 2013](#)). Moreover, this recovery is effected using an order-optimal number of random measurements ([Foucart and Rauhut, 2013](#)). In applications like medical imaging ([Adcock and Hansen, 2021](#)), the measurement matrices under consideration are derived from a bounded orthonormal system (a unitary matrix with bounded entries), which complicates the theoretical analysis. Furthermore, for such applications one desires a highly effective representation for encoding the images. Developing a theoretical analysis that properly accounts for realistic measurement paradigms and complexly designed image representations is non-trivial in general ([Bora et al., 2017](#); [Foucart and Rauhut, 2013](#); [Jalal et al., 2021](#)). For example, there has been much work validating that *generative neural networks* (GNNs) are highly effective at representing natural signals ([Goodfellow et al., 2014](#); [Kingma and Welling, 2013](#); [Radford et al., 2015](#)). In this vein, recent work has shown promising empirical results for compressed sensing with realistic measurement matrices when the structural proxy is a GNN. Other recent work has established recovery guarantees for compressed sensing when the structural proxy is a GNN and the measurement matrix is subgaussian ([Bora et al., 2017](#)). (See [Related work](#) for a fuller depiction of related aspects of this problem.) However, an open problem is the following ([Scarlett et al., 2022, p. 10](#)):

**Open problem** (subIso GCS). *A theoretical analysis of compressed sensing when the measurement matrix is structured (e.g., a randomly subsampled unitary matrix) and the signal model proxy is a GNN.*

Broadly, we approach a solution to [subIso GCS](#) as follows. For a matrix  $A \in \mathbb{C}^{m \times n}$ , a particular GNN *architecture*  $G : \mathbb{R}^k \rightarrow \mathbb{R}^n$  and an unknown signal  $x_0 \in \mathcal{R}(G)$ , the range of  $G$ , we determine the conditions (on  $A, G, x_0$ , etc.) under which it is possible to approximately recover  $x_0$  from noisy linear measurements  $b = Ax_0 + \eta$  by (approximately) solving an optimization problem of the form

$$\min_{z \in \mathbb{R}^k} \|b - AG(z)\|_2. \quad (1)$$

Above,  $\eta \in \mathbb{C}^m$  is some unknown corruption. Specifically, we are interested in establishing sample complexity bounds (lower bounds on  $m$ ) for realistic measurement matrices  $A$  — where  $A$  is an underdetermined matrix randomly subsampled from a unitary matrix. Namely, the rows of  $A$  have been sampled uniformly at random without replacement from a unitary matrix  $U \in \mathbb{C}^{n \times n}$ . We next present a mathematical description of the subsampling of the rows, described similarly to ([Dirksen, 2015](#), Section 4).

**Definition I.1** (subsampled isometry). Let  $2 \leq m \leq n < \infty$  be integers and let  $U \in \mathbb{C}^{n \times n}$  be a unitary matrix. Let  $\theta := (\theta_i)_{i \in [n]}$  be an iid Bernoulli random vector:  $\theta_i \stackrel{\text{iid}}{\sim} \text{Ber}(m/n)$ . Define the set  $\mathcal{J} := \{j : \theta_j = 1\}$  and enumerate the elements of  $\mathcal{J}$  as  $j_1, \dots, j_{\tilde{m}}$  where  $\tilde{m} := |\mathcal{J}|$  is a binomial random variable with  $\mathbb{E} \tilde{m} = m$ . Let  $A \in \mathbb{C}^{\tilde{m} \times n}$  be the matrix whose  $i$ th row is  $\frac{\sqrt{n}}{\sqrt{m}} U_{j_i}, i \in [\tilde{m}]$ . We call  $A$  an  $(m, U)$ -subsampled isometry. When there is no risk of confusion we simply refer to  $A$  as a subsampled isometry and implicitly acknowledge the existence of an  $(m, \theta, U)$  giving rise to  $A$ .

With  $A$  so defined,  $A$  is *isotropic*:  $\mathbb{E} A^* A = \sum_{i=1}^n U_i^* U_i = I_n$  where  $I_n$  is the  $n \times n$  identity matrix.

*Remark I.1.* An important example of a matrix isometry is the discrete orthogonal system given by the (discrete) Fourier basis. For example, “in applications such as medical imaging, one is confined to using subsampled Fourier measurements due to the inherent design of the hardware” (Scarlett et al., 2022, p. 10). Let  $F = (F_{ij})_{i,j \in [n]}$  with  $F_{ij} := \frac{1}{\sqrt{n}} \exp(2\pi i(i-1)(j-1)/n)$  for each  $i, j \in [n]$ . Here, we have used  $i$  to denote the complex number satisfying  $i^2 = -1$ . The matrix  $F$  is known as the discrete Fourier transform (DFT) matrix, and has important roles in signal processing and numerical computation (Adcock and Hansen, 2021; Jalal et al., 2021; Scarlett et al., 2022). Thus, all of our results apply, in particular, when the measurement matrix is a subsampled DFT.  $\diamond$

Lastly, we introduce the kind of GNN to which we restrict our attention in this work. Namely, we study ReLU-activated expansive neural networks, where ReLU is the so-called rectified linear unit defined as  $\sigma(x) := \max(x, 0)$ , acting element-wise on the entries of  $x$ .

**Definition I.2**  $((k, d, n)$ -generative network). Fix the integers  $2 \leq k := k_0 \leq k_1 \leq \dots \leq k_d =: n < \infty$  and suppose for  $i \in [d]$  that  $W^{(i)} \in \mathbb{R}^{k_i \times k_{i-1}}$ . A  $(k, d, n)$ -generative network is a function  $G : \mathbb{R}^k \rightarrow \mathbb{R}^n$  of the form

$$G(z) := W^{(d)} \sigma \left( \dots W^{(2)} \sigma \left( W^{(1)} z \right) \right).$$

With these ingredients, we provide a suggestive “cartoon” of the main theoretical contribution of this work, which itself can be found in [Theorem II.1](#).

**Theorem Sketch** (Cartoon). *Let  $G$  be a  $(k, d, n)$ -generative network, and  $A$  a subsampled isometry. Suppose  $\mathcal{R}(G) - \mathcal{R}(G)$  is “incoherent” with respect to the rows of  $A$ , quantified by a parameter  $\alpha > 0$ . If the number of measurements  $m$  satisfies  $m \gtrsim kn\alpha^2 \log n$ , then, with high probability on  $A$ , it is possible to approximately recover an unknown signal  $x_0 \in \mathcal{R}(G)$  from noisy undetermined linear measurements  $b = Ax_0 + \eta$  with nearly order-optimal error.*

Coherence is defined in [Definition I.4](#) below, using the *measurement norm* introduced in [Definition I.3](#). The notion of “incoherence” in the cartoon above is specified in [Corollary II.3](#). Coherence is related to the concept of incoherent bases (Foucart and Rauhut, 2013, p. 373), while the measurement norm is closely related to the so-called  $X$ -norm in Rudelson and Vershynin (2008). Effectively, coherence characterizes

the alignment between the components comprising  $\mathcal{R}(G)$  and the row vectors  $A_i$  of the subsampled isometry  $A$ .

**Definition I.3** (Measurement norm). Let  $U \in \mathbb{C}^{n \times n}$  be a unitary matrix. Define the norm  $\|\cdot\|_U : \mathbb{C}^n \rightarrow [0, \infty)$  by

$$\|x\|_U := \|Ux\|_\infty = \max_{i \in [n]} |\langle U_i, x \rangle|.$$

**Definition I.4** (Coherence). Let  $T \subseteq \mathbb{R}^n$  be a set and  $U \in \mathbb{C}^{n \times n}$  a unitary matrix. For  $\alpha > 0$ , say that  $T$  is  $\alpha$ -coherent with respect to  $\|\cdot\|_U$  if

$$\sup_{x \in T \cap \mathbb{S}^{n-1}} \|x\|_U \leq \alpha.$$

We refer to the quantity on the left-hand side as *the coherence*.

The idea is that the structural proxy/prior under consideration should be *incoherent* with respect to the measurement process. Thus, we desire that vectors in  $\mathcal{R}(G)$  be not too closely aligned (in the sense controlled by  $\alpha$ ) with the rows of  $U$ , to which the subsampled isometry  $A$  is associated. We argue that this is a natural quantity to consider. Though it is likely difficult to measure precisely in practice, we propose a computationally efficient heuristic that upper bounds the coherence. Furthermore, we propose, under suitable randomness assumptions, that an assumed bound on the coherence may be considered rather mild. Loosely: if  $G$  has Gaussian weights, one may take  $\alpha^2 \sim kd/n$  in [Cartoon](#) (see [Theorem II.1](#) and [Theorem III.2](#)).

We briefly itemize the main contributions of this paper:

- we introduce the *coherence* for characterizing recovery efficacy via the alignment of the network’s range with the measurement matrix (see [Definition I.4](#));
- we establish a restricted isometry property for  $(k, d, n)$ -generative networks with subsampled isometries (see [Theorem II.2](#) and [Corollary II.3](#));
- we prove sample complexity and recovery bounds in this setting (see [Theorem II.1](#));
- we propose a regularization strategy for training GNNs with low coherence (see [§ IV-A](#)) and demonstrate improved sample complexity for recovery (see [§ IV-B](#));
- together with our theory, we provide compelling numerical simulations that support coherence as a natural quantity of interest linked to favourable deep generative recovery (see [§ IV-B](#)).

## A. Related work

Theoretically, Bora et al. (2017) have analyzed compressed sensing problems in the so-called generative prior framework, focusing on Gaussian or subgaussian measurement matrices. Similar problems in the generative prior framework have been analyzed, but all have relied on random designs to our knowledge. For example, Berk (2021) extends the analysis to the setting of demixing with subgaussian matrices, while Liu and Liu (2022) analyzes the semi-parametric single-index model with generative prior under Gaussian measurements. Finally, exact recovery of the underlying latent code for GNNs (*i.e.*, seeking  $z \in \mathbb{R}^k$  such that  $x = G(z)$ ) has been analyzed; however, these analyses rely on the GNN having a

suitable structure with weight matrices that possess a suitable randomness (Hand and Joshi, 2019; Hand and Voroninski, 2019; Hand et al., 2018; Joshi et al., 202book1). For a review of these and related problems, see Scarlett et al. (2022).

Promising empirical results of Jalal et al. (2021) suggest remarkable efficacy of generative compressed sensing (GCS) in realistic measurement paradigms. Furthermore, the authors provide a framework with theoretical guarantees for using Langevin dynamics to sample from a generative prior. Several recent works have developed sophisticated generative adversarial networks (GANs) (which are effectively a type of GNN) for compressed sensing in medical imaging (Deora et al., 2020; Mardani et al., 2018). Other work has empirically explored multi-scale (non-Gaussian) sampling strategies for image compressed sensing using GANs (Li et al., 2022). Separately, see Wentz and Doostan (2022) for the use of GCS in uncertainty quantification of high-dimensional partial differential equations with random inputs. Recently popular is the use of untrained GNNs for signal recovery (Heckel and Hand, 2019; Ulyanov et al., 2018). For instance, Darestani and Heckel (2021) executed a promising empirical investigation of medical image compressed sensing using untrained GNNs.

Compressed sensing with subsampled isometries is well studied for sparse signal recovery. The original works developing such recovery guarantees are Candès et al. (2006); Donoho (2006), with improvements appearing in Rauhut (2010); Rudelson and Vershynin (2008). See Foucart and Rauhut (2013) for a thorough presentation of this material including relevant background. See Dirksen (2015, Sec. 4) for a clear presentation of this material via an extension of generic chaining. In this setting, the best-known number of log factors in the sample complexity bound sufficient to achieve the restricted isometry property is due to Bourgain (2014) with subsequent extensions and improvements in (Brugliapaglia et al., 2021; Chkifa et al., 2018; Haviv and Regev, 2017). Naderi and Plan (2022) address compressed sensing with subsampled isometries when the structural proxy is a neural network with random weights.

Using a notion of coherence to analyze the solution of convex linear inverse problems was proposed in Candès and Romberg (2007); Candès et al. (2006). Cape et al. (2019) relate this notion to the matrix norm  $\|\cdot\|_{2 \rightarrow \infty}$  (defined in **Notation**) in order to analyze covariance estimation and singular subspace recovery. Additionally, see Donoho and Elad (2003) or Foucart and Rauhut (2013, p. 373) for a discussion of *incoherent bases*, and Rudelson and Vershynin (2008, p. 1034) for the analogue of our measurement norm in the sparsity case.

The present work relies on important ideas from high-dimensional probability, such as controlling the expected supremum of a random process on a geometric set. These ideas are well treated in Jeong et al. (2020); Liaw et al. (2017); see Vershynin (2018) for a thorough treatment of high-dimensional probability. This work also relies on counting linear regions comprising the range of a ReLU-activated GNN. In this respect, we rely on a result that appears in Naderi and Plan (2021). Tighter but less analytically tractable bounds appear in (Serra et al., 2018), while a computational exploration of region counting has been performed in Novak et al. (2018).

## B. Notation

For an integer  $n \geq 1$  denote  $[n] := \{1, \dots, n\}$ . For  $x \in \mathbb{C}^n$ , denote the  $\ell_p$  norm for  $1 \leq p < \infty$  by  $\|x\|_p := (\sum_{i=1}^n |x_i|^p)^{1/p}$  and for  $p = \infty$  by  $\|x\|_\infty := \max_{i \in [n]} |x_i|$ . Here, if  $x \in \mathbb{C}$  then  $|x| = \sqrt{\operatorname{Re}(x)^2 + \operatorname{Im}(x)^2}$  and the conjugate is given by  $\bar{x} := \operatorname{Re}(x) - i\operatorname{Im}(x)$ . If  $X \in \mathbb{C}^{m \times n}$  is a matrix then the conjugate transpose is denoted  $X^* = (\bar{X}_{ji})_{j \in [n], i \in [m]}$ . The  $\ell_p$  norm for real numbers,  $1 \leq p \leq \infty$  is defined in the standard, analogous way. Denote the real and complex sphere each by  $\mathbb{S}^{n-1} := \{x : \|x\|_2 = 1\}$ , disambiguating only where unclear from context. The operator norm of a matrix  $X \in \mathbb{C}^{n \times n}$ , induced by the Euclidean norm, is denoted  $\|X\| := \sup_{\|z\|_2=1} \|Xz\|_2$ . Unless otherwise noted,  $X_i$  denotes the  $i$ th row of the matrix  $X$ , viewed as a column vector. The Frobenius norm of  $X$  is denoted  $\|X\|_F$  and satisfies  $\|X\|_F^2 = \sum_{i=1}^m \|X_i\|_2^2$ . The matrix norm  $\|\cdot\|_{p \rightarrow q}$  for  $1 \leq p, q \leq \infty$  is  $\|X\|_{p \rightarrow q} := \sup_{z \neq 0} \frac{\|Xz\|_q}{\|z\|_p}$ . We use  $\Pi_{\mathcal{L}}$  to denote the standard  $\ell_2$  projection operator onto the set  $\mathcal{L}$ , which selects a single point lexicographically, if necessary, to ensure uniqueness.  $\operatorname{Ber}(p)$  denotes the Bernoulli distribution with parameter  $p$ ;  $\operatorname{Binom}(n, p)$  the binomial distribution for  $n$  items with rate  $p$ .

Throughout this work,  $C > 0$  represents an absolute constant having no dependence on any parameters, whose value may change from one appearance to the next. Constants with dependence on a parameter will be denoted with an appropriate subscript — e.g.,  $C_\delta$  is an absolute constant depending only on a parameter  $\delta$ . Likewise, for two quantities  $a, b$ , if  $a \lesssim b$  then  $a \leq Cb$ ; analogously for  $a \gtrsim b$ . Finally, given two sets  $A, B \subseteq \mathbb{R}^n$ ,  $A \pm B$  denotes the Minkowski sum/difference:  $A \pm B := \{a \pm b : a \in A, b \in B\}$ . Similarly, for  $a \in \mathbb{R}^n$ ,  $a - B := \{a - b : b \in B\}$  and  $aB := \{ab : b \in B\}$ . The range of a function  $f : \mathbb{R}^n \rightarrow \mathbb{R}^m$  is denoted  $\mathcal{R}(f) := \{f(x) : x \in \mathbb{R}^n\}$  (e.g., if  $X$  is a matrix then  $\mathcal{R}(X)$  denotes the column space of  $X$ ).

## II. MAIN RESULTS

We start by presenting the main result of the paper, which establishes sample complexity and recovery bounds for generative compressed sensing with subsampled isometries. Below,  $x^\perp := x_0 - \Pi_{\mathcal{R}(G)} x_0$ .

**Theorem II.1** (subsampled isometry GCS). *Let  $G : \mathbb{R}^k \rightarrow \mathbb{R}^n$  be a  $(k, d, n)$ -generative network and  $A \in \mathbb{C}^{\tilde{m} \times n}$  a subsampled isometry associated to a unitary matrix  $U \in \mathbb{C}^{n \times n}$ . If  $\mathcal{G} := \mathcal{R}(G) - \mathcal{R}(G)$  is  $\alpha$ -coherent with respect to  $\|\cdot\|_U$ , and*

$$m \gtrsim \frac{\alpha^2 n}{\delta^2} \left( 2k \sum_{i=1}^{d-1} \log \left( \frac{2ek_i}{k} \right) + \log \frac{4k}{\varepsilon} \right),$$

*then, the following holds with probability at least  $1 - \varepsilon$  on the realization of  $A$ .*

*For any  $x_0 \in \mathbb{R}^n$ , let  $b := Ax_0 + \eta$  where  $\eta \in \mathbb{C}^{\tilde{m}}$ . If*

$$x_* \in \arg \min_{x \in \mathcal{R}(G)} \|b - Ax\|_2,$$

and  $\hat{x} \in \mathcal{R}(G)$  satisfies  $\|b - A\hat{x}\|_2 \leq \|b - Ax_*\|_2 + \varepsilon$ , then,

$$\begin{aligned} \|x_0 - \hat{x}\|_2 &\leq \frac{5+3\delta}{1-\delta} \|x_* - x_0\|_2 \\ &\quad + \frac{1}{1-\delta} (2\|\eta\|_2 + \varepsilon + 2\|Ax^\perp\|_2). \end{aligned}$$

**Remark II.1.** The *modelling error* incurred via  $\|Ax^\perp\|_2$  could be large compared to  $\|x^\perp\|_2$ . Generally, it holds that  $\|Ax^\perp\|_2 \leq \frac{\sqrt{n}}{\sqrt{m}} \|x^\perp\|_2$ . However, if  $G$  admits a good representation of the modelled data distribution, then one might expect this term still to be small. Certainly, if  $x_0 \in \mathcal{R}(G)$ , the final expression in **Theorem II.1** reduces to

$$\|\hat{x} - x_0\|_2 \leq \frac{5+3\delta}{1-\delta} \|x_* - x_0\|_2 + \frac{2\|\eta\|_2 + \varepsilon}{1-\delta}.$$

Otherwise, if  $x^\perp$  is independent of  $A$ ,  $\mathbb{E} \|Ax^\perp\|_2 \leq \|x^\perp\|_2$  by Jensen's inequality. Thus, by Markov's inequality one has  $\mathbb{P}\{\|Ax^\perp\|_2 \geq \kappa\|x^\perp\|_2\} \leq \kappa^{-1}$ . Finally, a strategy for more precisely controlling  $\|Ax^\perp\|_2$  is given in § C (see especially **Proposition A.5**).  $\diamond$

Analogous to the restricted isometry property of compressed sensing or the set-restricted eigenvalue condition of [Bora et al. \(2017\)](#), the proof of **Theorem II.1** relies on a restricted isometry condition. This condition guarantees when pairwise distances of points in  $\mathcal{R}(G)$  are approximately preserved under the action of  $A$ . We first state a result controlling norms of points in  $\mathcal{R}(G)$  under the action of  $A$ ; control over pairwise distances then follows easily.

**Theorem II.2** (Gen-RIP). *Let  $A \in \mathbb{C}^{\tilde{m} \times n}$  be a subsampled isometry associated to a unitary matrix  $U \in \mathbb{C}^{n \times n}$ . Suppose that  $G : \mathbb{R}^k \rightarrow \mathbb{R}^n$  is a  $(k, d, n)$ -generative network and that  $\mathcal{R}(G)$  is  $\alpha$ -coherent with respect to  $\|\cdot\|_U$ . If*

$$m \gtrsim \frac{\alpha^2 n}{\delta^2} \left( k \sum_{i=1}^{d-1} \log \left( \frac{2ek_i}{k} \right) + \log \frac{2k}{\varepsilon} \right),$$

then with probability at least  $1 - \varepsilon$  on the realization of  $A$ , it holds that

$$\sup_{x \in \mathcal{R}(G) \cap \mathbb{S}^{n-1}} |\|Ax\|_2 - 1| \leq \delta.$$

**Remark II.2.** The above result is interesting when  $\alpha = \alpha(n) = \mathcal{O}(n^{-1/2})$ . In § III we argue that such dependence is possible (see **Proposition III.1** and **Theorem III.2**).  $\diamond$

We now state the result that provides the notion of restricted isometry needed for **Theorem II.1**. This result, which controls pairwise differences of elements in  $\mathcal{R}(G)$ , is an immediate consequence of **Theorem II.2** using the observation in **Remark A.3**.

**Corollary II.3** (Restricted isometry on the difference set). *Let  $G : \mathbb{R}^k \rightarrow \mathbb{R}^n$  be a  $(k, d, n)$ -generative network and suppose  $A \in \mathbb{C}^{\tilde{m} \times n}$  is a subsampled isometry associated to a unitary matrix  $U \in \mathbb{C}^{n \times n}$ . Assume that  $\mathcal{G} := \mathcal{R}(G) - \mathcal{R}(G)$  is  $\alpha$ -coherent with respect to  $\|\cdot\|_U$ . If*

$$m \gtrsim \frac{\alpha^2 n}{\delta^2} \left( 2k \sum_{i=1}^{d-1} \log \left( \frac{2ek_i}{k} \right) + \log \frac{4k}{\varepsilon} \right),$$

then with probability at least  $1 - \varepsilon$  on the realization of  $A$ , it holds that

$$\sup_{x \in \mathcal{G} \cap \mathbb{S}^{n-1}} |\|Ax\|_2 - 1| \leq \delta.$$

The proofs of **Theorem II.2** and **Theorem II.1** are deferred to § V-A. The result **Theorem II.2** follows directly from **Lemma II.4** and **Lemma A.4**, the former of which is presented next. It characterizes restricted isometry of a subspace incoherent with  $\|\cdot\|_U$ . Its proof is deferred to § V-A.

**Lemma II.4** (RIP for incoherent subspace). *Let  $A \in \mathbb{C}^{\tilde{m} \times n}$  be a subsampled isometry associated to a unitary matrix  $U \in \mathbb{C}^{n \times n}$  and suppose that  $\mathcal{L} \subseteq \mathbb{R}^n$  is a  $k$ -dimensional subspace that is  $\alpha$ -coherent with respect to  $\|\cdot\|_U$ . Then, for any  $\delta \geq 0$ ,*

$$\mathbb{P} \left\{ \sup_{x \in \mathcal{L} \cap \mathbb{S}^{n-1}} |\|Ax\|_2 - 1| \geq \delta \right\} \leq 2k \exp \left( - \frac{C\delta^2 m}{\alpha^2 n} \right).$$

**Remark II.3.** Convincing empirical results of [Novak et al. \(2018\)](#) suggest the number of linear regions for empirically observed neural networks may typically be linear in the number of nodes, rather than exponential in the width. Such a reduction would be a boon for the sample complexity obtained in **Theorem II.2**, which depends on the number of linear regions comprising  $\mathcal{R}(G)$  (using **Lemma A.4**; see § V-A).  $\diamond$

### III. TYPICAL COHERENCE

The first result of this section establishes a lower bound on the coherence parameter yielding a quadratic “bottleneck” on the sample complexity in terms of the parameter  $k$ .

**Proposition III.1.** *Let  $U \in \mathbb{C}^{n \times n}$  be a unitary matrix. Any  $k$ -dimensional subspace  $T \subseteq \mathbb{R}^n$  is at least  $\sqrt{\frac{k}{n}}$ -coherent with respect to  $\|\cdot\|_U$ . Furthermore, this lower bound is tight.*

Under mild assumptions, when the generative network has random weights one may show that this is a typical coherence level between the network and the measurement operator.

**Theorem III.2.** *Let  $U \in \mathbb{C}^{n \times n}$  be a unitary matrix and  $G$  be a  $(k, d, n)$ -generative network. Assume the weight matrices of  $G$ ,  $W^{(\ell)}$ ,  $\ell \in [d]$ , are jointly iid Gaussian:  $W_{ij}^{(\ell)} \stackrel{iid}{\sim} \mathcal{N}(0, 1)$ ,  $i \in [k_\ell]$ ,  $j \in [k_{\ell-1}]$ . Then, with probability at least  $1 - 2\exp(-\gamma^2)$ ,  $\mathcal{R}(G) - \mathcal{R}(G)$  is  $\alpha$ -coherent with respect to  $\|\cdot\|_U$ , where*

$$\alpha \leq \sqrt{\frac{k}{n}} + \sqrt{\frac{\log n}{n}} + \sqrt{\frac{k}{n} \sum_{i=1}^{d-1} \log \frac{2ek_i}{k} + \frac{\gamma}{\sqrt{n}}}.$$

**Remark III.1.** We briefly comment on the behaviour of the third term, which, we argue, dominates for the principal case of interest. Assume the layers have approximately constant size: *i.e.*, for two absolute constants  $C_1, C_2 > 0$ ,

$$\forall \ell \in [d], \quad C_1 \leq \log \frac{ek_\ell}{k} \leq C_2.$$

In this case, all terms in the sum in the third term will be of the same order, making this term have order  $\mathcal{O}(\sqrt{\frac{kd}{n}})$ . If

we further make the reasonable assumption that  $dk > \log(n)$ , then the third term dominates all others, hence

$$\alpha = \mathcal{O}\left(\sqrt{\frac{kd}{n}}\right).$$

◇

**Remark III.2.** Using [Corollary II.3](#) and [Remark III.1](#), one may take as the sample complexity for [Theorem II.1](#), in the case of a  $(k, d, n)$ -generative network with Gaussian weights,

$$m \gtrsim \frac{2k^2d}{\delta^2} \sum_{i=1}^{d-1} \log\left(\frac{2ek_i}{k}\right) + \frac{kd}{\delta^2} \log\frac{4k}{\varepsilon}.$$

◇

#### IV. NUMERICS

In this section we explore the connection between coherence and recovery error empirically, to suggest that coherence is indeed the salient quantity dictating recovery error. In addition, we propose a regularization strategy to train low coherence GNNs. This regularization strategy is new to our knowledge. The first experiment illustrates a phase portrait that empirically shows dependence on coherence and number of measurements for successful recovery. We also show, for a fixed number of measurements, that the probability of recovery failure increases with higher coherence. In the second experiment, we use the novel regularization approach to show that fewer measurements are required for signal recovery when a GNN is trained to have low coherence.

##### A. Experimental methodology

*1) Coherence heuristic and regularization:* Ideally, in these experiments, one would calculate the coherence of the network exactly, via [Definition I.4](#). However, computing coherence is likely intractable in general. Instead, we use an upper bound on the coherence obtained as follows. Let  $G$  be a  $(k, d, n)$ -generative network and let  $W = W^{(d)}$  be its final weight matrix. Write the QR decomposition of  $W$  as

$$W = QR, \quad Q := \begin{bmatrix} Q_1 & Q_2 \end{bmatrix}, \quad R := \begin{bmatrix} R_1 \\ 0 \end{bmatrix},$$

where  $Q \in \mathbb{R}^{n \times n}$  is orthogonal,  $R \in \mathbb{R}^{n \times \tilde{k}}$  has invertible submatrix  $R_1 \in \mathbb{R}^{\tilde{k} \times \tilde{k}}$  and  $Q_1 \in \mathbb{R}^{\tilde{n} \times \tilde{k}}$  is the submatrix multiplying with  $R_1$ . Let  $\mathcal{G} := (\mathcal{R}(G) - \mathcal{R}(G)) \cap \mathbb{S}^{n-1}$ ,  $\mathcal{W} := \mathcal{R}(W) \cap \mathbb{S}^{n-1}$  and let  $D \in \mathbb{R}^{n \times n}$  be an orthogonal matrix. Using that  $\mathcal{G} \subseteq \mathcal{W}$ , we bound the coherence with respect to  $\|\cdot\|_D$  as

$$\begin{aligned} \sup_{x \in \mathcal{G}} \|Dx\|_\infty &\leq \sup_{x \in \mathcal{W}} \|Dx\|_\infty \\ &= \max_{i \in [n]} \sup_{z \in \mathbb{R}^{\tilde{k}}} \{|D_i^\top QRz| : \|Rz\|_2 = 1\} \\ &= \max_{i \in [n]} \sup_{v \in \mathbb{R}^{\tilde{k}}} \{|D_i^\top Q_1 v| : \|v\|_2 = 1\} \\ &= \max_{i \in [n]} \|Q_1^\top D_i\|_2 = \|DQ_1\|_{2 \rightarrow \infty}, \end{aligned} \quad (2)$$

where the penultimate line uses  $z := R_1^{-1}v$ . To re-phrase: a network  $G$  is always  $\|DQ_1\|_{2 \rightarrow \infty}$ -coherent with respect to

$\|\cdot\|_D$ . Our experiments and theory are consistent with the hypothesis that this is an effective heuristic for coherence.

Motivated by (2), we propose a strategy — novel, to our knowledge — to promote low coherence of the final layer  $W$  with respect to a fixed orthogonal matrix  $D$ . This is achieved by applying the following regularization  $\rho$  to the final weight matrix of the GNN during training:

$$\rho(W) = \|DW\|_{2 \rightarrow \infty} + \|W^\top W - I\|_F. \quad (3)$$

Namely, the regularizer  $\rho$  is added to the training loss function. Roughly, this regularization promotes low coherence because  $\|W^\top W - I\|_F$  is smallest when  $W$  is orthonormal, making  $\|DW\|_{2 \rightarrow \infty}$  the coherence of  $\mathcal{R}(W)$  with respect to  $D$ .

*2) Network architectures:* In the experiments, we use three generative neural networks trained on the MNIST dataset ([Deng, 2012](#)), which consists of 60,000  $28 \times 28$  images of handwritten digits. The GNNs are fully connected networks with three layers and parameters  $k = 20$ ,  $k_1 = k_2 = 500$ ,  $n = 784$ . Precisely, let the first one be  $G^{(1)} = s(W^{(1,3)}\sigma(W^{(1,2)}\sigma(W^{(1,1)}z)))$ , where  $s(x) = (1 + \exp(-x))^{-1}$  is the sigmoid activation function. Let the remaining two GNNs be  $G^{(i)}(z) = W^{(i,3)}\sigma(W^{(i,2)}\sigma(W^{(i,1)}z))$ ,  $i = 2, 3$ . We use  $G^{(1)}$ , which has a more realistic architecture for real applications, as a point of comparison with  $G^{(i)}$ ,  $i = 2, 3$ . Variational autoencoders (VAEs) ([Kingma and Welling, 2013](#)), with the decoder network as  $G^{(1)}$  and  $G^{(2)}$ , were trained using the Adam optimizer ([Kingma and Ba, 2014](#)) with a learning rate of 0.001 and a mini-batch size of 64 using Flux ([Innes, 2018](#)). We trained another VAE with decoder network  $G^{(3)}$ , using the same hyperparameters but using the regularization strategy described in § IV-A1 to promote low coherence of the final layer  $W^{(3,3)}$  with respect to a fixed orthogonal matrix  $D$ . Specifically, the expression  $10^4\rho(W^{(3,3)})$  was added to the VAE loss function. In all cases the VAE loss function was the usual one. See the [code repository](#) for specific implementation details including the definition of the encoders, and refer to ([Kingma and Welling, 2013; 2019](#)) for further background on VAEs.

*3) Measurement matrix:* Throughout the experiments, the matrix  $D$  was chosen to be the discrete cosine transform (DCT) matrix. For DCT implementation details, see for instance [Virtanen et al. \(2020, fftpack.dct\)](#). The matrix  $A$  is a mild variant of the subsampled isometry defined in [Definition I.1](#), modified to ensure that each realization of  $A$  has  $m$  rows. Namely, the random matrix  $A$  is subsampled from  $D$  by selecting the first  $m$  elements of a uniform random permutation of  $[n]$ . Note  $A$  is still re-normalized as in [Definition I.1](#).

*4) First experiment:* For the first experiment, let  $G_\beta$  be a  $(k, 2, n)$ -generative network with inner layers  $W^{(i)} = W^{(1,i)}$ ,  $i = 1, 2$  and last layer  $W^{(3)} = W_\beta \in \mathbb{R}^{n \times \tilde{k}}$  defined by

$$W_\beta := \beta W^{(1,3)} + (1 - \beta)W^{(3,3)}.$$

Recall that  $W^{(1,3)}$  and  $W^{(3,3)}$  are the final layers of  $G^{(1)}$  and  $G^{(3)}$ , respectively. Here,  $\beta \in [0, 1]$  is an interpolation parameter. The coherence of  $\mathcal{R}(W^{(1,3)})$  was 0.98, while the coherence of  $G^{(3)}$  was upper bounded via (2) as 0.82. As

a result, for large  $\beta$ , one should expect  $W_\beta$  to have large coherence with respect to  $\|\cdot\|_D$ . We randomly sample  $z_0 \in \mathbb{R}^k$ , fix the number of measurements  $m \in \{40, 60, \dots, 440\}$ , and set  $b = AG_\beta(z_0)$ . For each measurement size  $m$  and coherence upper bound, we perform 20 independent trials. For each trial, we approximately solve (1) by running ADAM with a learning rate of 0.1 for 5000 iterations, or until the norm of the gradient is less than  $10^{-7}$ , and set  $\hat{z}$  to be the output. See the [code repository](#) for specific implementation details. We say the target signal  $G_\beta(z_0)$  was successfully recovered if the relative reconstruction error (rre) between  $G_\beta(z_0)$  and  $G_\beta(\hat{z})$  is less than  $10^{-5}$ :

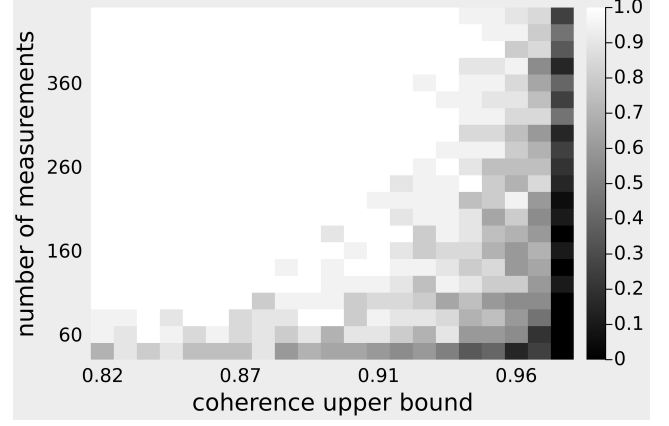
$$\text{rre}(x_0, \hat{x}) := \frac{\|x_0 - \hat{x}\|_2}{\|x_0\|_2}.$$

5) *Second experiment:* For the second experiment, we use each trained network  $G^{(i)}$ ,  $i = 1, 2, 3$ . The coherence upper bounds of  $G^{(2)}$  and  $G^{(3)}$ , computed using (2) are 0.96 and 0.81, respectively, which empirically shows that the regularization (3) promotes low coherence during training. For the networks  $G^{(i)}$ , let  $E^{(i)} : \mathbb{R}^n \rightarrow \mathbb{R}^k$  be the corresponding encoder network from their shared VAE. We randomly sample an image  $x^\sharp$  from the test set of the MNIST dataset and let  $x_0^{(i)} = G^{(i)}(E^{(i)}(x^\sharp))$  — i.e.,  $x_0^{(i)} \in \mathcal{R}(G^{(i)})$  most likely resembles the test set image  $x^\sharp$ . Let  $m \in \{10, 15, 20, 25, 50, 100, 200, 250\}$  and set  $b^{(i)} = Ax_0^{(i)}$ . For each measurement size  $m$ , we run 10 independent trials. On each trial, we generate a realization of  $A$  and randomly sample a test image  $x^\sharp$  from the MNIST dataset. To estimate  $x_0^{(i)}$  on each trial, we approximately solve (1) by running ADAM with a learning rate of 0.1 for 5000 iterations, or until the Euclidean norm of the gradient is less than  $10^{-7}$ . See the [Berk et al. \(2022\)](#) for specific implementation details.

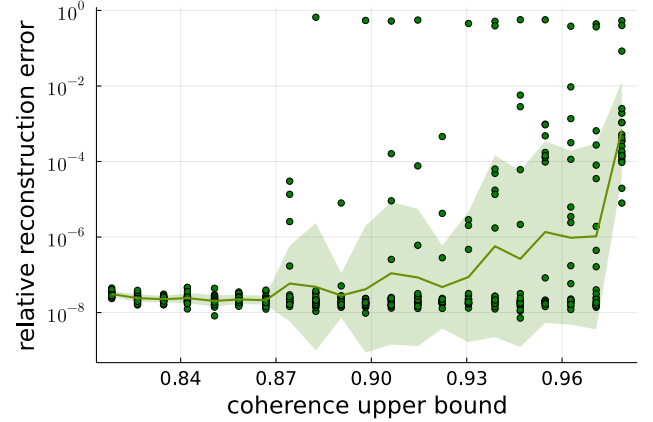
## B. Numerical results

1) *Recovery phase transition:* The results of the first experiment appear in [Figure 1](#). Specifically, [Figure 1a](#) plots the fraction of successful recoveries from 20 independent trials as a function of the coherence heuristic (2) and number of measurements. White squares correspond to 100% successful recovery (all errors were below  $10^{-5}$ ), while black squares correspond to no successful recoveries (all errors were above  $10^{-5}$ ). In [Figure 1b](#), we show a slice of the phase plot for  $m = 100$ , plotting rre as a function of the coherence heuristic (2). Each dot corresponds to one of 20 trials at each coherence level. The plot is shown on a log- $y$  scale. The solid line plots the geometric mean of rre as a function of coherence, with an envelope representing 1 geometric standard deviation (see [Adcock et al. \(2022, App. A.1.3\)](#) for more information on this visualization strategy). [Figure 1](#) indicates that coherence may be effectively controlled via the heuristic (2), and that coherence is a natural quantity associated with recovery performance. These findings corroborate our theoretical results.

2) *Incoherent networks require fewer measurements:* In the second experiment, we provide compelling numerical simulations that support our regularization strategy for lowering coherence of the trained network, resulting in stable recovery



(a) Empirical recovery probability as a function of coherence and  $m$ . Each block corresponds to the average from 20 independent trials. White corresponds with 20 successful recoveries ( $\text{rre} \leq 10^{-5}$ ); black with no successful recoveries.



(b) Empirical rre as a function of coherence for  $m = 100$ . Each dot corresponds to one of 20 trials at each coherence level. The solid line shows the empirical geometric mean rre vs. coherence upper bound. The envelope shows 1 geometric standard deviation.

Fig. 1: Dependence of recovery on coherence and number of measurements  $m$  for GNNs trained on MNIST.

of the target signal with much fewer measurements. The results of the second experiment are shown in [Figure 2](#) and [Figure 3](#). In [Figure 2](#), we show the recovered image for three images from the MNIST test set. For each block of  $3 \times 9$  images, the top row corresponds with the low coherence  $G^{(3)}$  ( $\alpha = 0.82$ ); the middle row, the high coherence  $G^{(2)}$  ( $\alpha = 0.96$ ); and the bottom row,  $G^{(1)}$ , which uses sigmoid activation. The left-most column is the target image belonging to  $\mathcal{R}(G^{(i)})$ , labelled *signal*. All images were *clamped* to the range  $[0, 1]$ . The figure shows that a GNN with low coherence can effectively recover the target signal with much fewer measurements compared to a network with high coherence, even when that network uses a final sigmoid activation function (which is a realistic choice in practical settings). Remarkably, in some cases we observed that images could be recovered with fewer than  $k$  measurements. This highlights the importance of regularizing for networks with low coherence during training. In [Figure 3](#), we further provide empirical evidence of the benefit of low coherence for recovery. For each measurement, we show the



Fig. 2: Recovery comparison of MNIST images for various measurement sizes  $m$  (denoted by column heading) for a low coherence network, high-coherence network and network with final sigmoid activation. In each block: the top row corresponds to  $G^{(3)}$  ( $\alpha = 0.82$ ); middle row  $G^{(2)}$  ( $\alpha = 0.96$ ); bottom row  $G^{(1)}$  (labelled Sig). The leftmost column, signal, corresponds to the target image  $x_0^{(i)} \in \mathcal{R}(G^{(i)})$ .

results of 10 independent trials for  $G^{(1)}$  (squares),  $G^{(2)}$  (triangles) and  $G^{(3)}$  (circles), respectively. The lines correspond to the empirical geometric mean rre for each network: the dotted line is associated with  $G^{(1)}$ ; the dashed line, the high coherence  $G^{(2)}$  ( $\alpha = 0.96$ ); and the solid line, the low coherence  $G^{(3)}$  ( $\alpha = 0.82$ ). The data are plotted on a log- $y$  scale. Each shaded envelope corresponds to 1 geometric standard deviation about the respective geometric means. This figure empirically supports that high probability successful recovery is achieved with markedly lower sample complexity for the lower coherence network  $G^{(3)}$ , as compared with either  $G^{(2)}$  or  $G^{(1)}$ . This finding corroborates our theoretical results.

## V. PROOFS

### A. Proofs for Main results

We proceed by proving [Theorem II.2](#), then [Theorem II.1](#). Note that [Corollary II.3](#), needed for [Theorem II.1](#), follows immediately from [Theorem II.2](#) using [Remark A.3](#).  $\square$

*Proof of Theorem II.2.* It follows from [Lemma A.4](#) that  $\mathcal{R}(G)$  may be contained in a union of  $N$  linear subspaces of

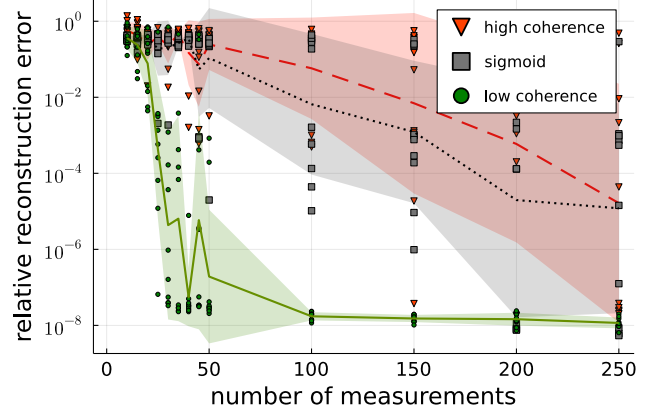


Fig. 3: Performance comparison for three GNNs trained on the MNIST dataset — one with low coherence, another with high coherence, and the last with sigmoid activation on the last layer. Plotted against number of measurements  $m$  is rre. For each value of  $m$ , each dot corresponds to one of 10 trials. In each trial, a random image drawn from the MNIST test partition was used as the target signal. Lines depict the empirical geometric mean rre as a function of  $m$ ; shaded regions correspond to 1 geometric standard deviation. The solid line corresponds to  $G^{(3)}$ ; the dashed line to  $G^{(2)}$ ; the dotted line to  $G^{(1)}$ .

dimension at most  $k$ ,  $\mathcal{R}(G) \subseteq \bigcup_{i=1}^N \mathcal{L}_i$ , with  $N$  satisfying

$$\log N \leq k \sum_{i=1}^{d-1} \log \left( \frac{2ek_i}{k} \right)$$

via [Remark A.2](#). For any linear subspace  $\mathcal{L}$  in the collection, observe that  $\mathcal{L}$  is  $\alpha$ -coherent with respect to  $\|\cdot\|_U$  by assumption. Consequently, by a union bound,

$$\begin{aligned} & \mathbb{P} \left\{ \sup_{x \in \mathcal{R}(G) \cap \mathbb{S}^{n-1}} |\|Ax\|_2 - 1| \geq \delta \right\} \\ & \leq \sum_{i=1}^N \mathbb{P} \left\{ \sup_{x \in \mathcal{L}_i \cap \mathbb{S}^{n-1}} |\|Ax\|_2 - 1| \geq \delta \right\} \\ & \leq 2Nk \exp \left( - \frac{Cm\delta^2}{\alpha^2 n} \right). \end{aligned}$$

The latter quantity is bounded above by  $\varepsilon$  if

$$m \gtrsim \frac{\alpha^2 n}{\delta^2} \left( \log N + \log \frac{2k}{\varepsilon} \right),$$

whence, by substituting the bound for  $\log N$ , it suffices to take

$$m \gtrsim \frac{\alpha^2 n}{\delta^2} \left( k \sum_{i=1}^{d-1} \log \left( \frac{2ek_i}{k} \right) + \log \frac{2k}{\varepsilon} \right).$$

*Proof of Theorem II.1.* With probability at least  $1 - \varepsilon$  on the realization of  $A$ ,  $A$  satisfies a restricted isometry condition on

the difference set  $\mathcal{R}(G) - \mathcal{R}(G)$  by [Corollary II.3](#). Therefore, since  $\hat{x}, x_* \in \mathcal{R}(G)$ ,

$$\|\hat{x} - x_*\|_2 \leq \frac{1}{1 - \delta} \|A(\hat{x} - x_*)\|_2$$

In particular, since  $\|b - Ax\|_2 \leq \|b - Ax_*\|_2 + \varepsilon$ ,

$$\begin{aligned} \|\hat{x} - x_*\|_2 &\leq \frac{1}{1 - \delta} (\|b - Ax_*\|_2 + \|Ax - b\|_2) \\ &\leq \frac{1}{1 - \delta} (2\|A(x_* - x_0)\|_2 + \varepsilon + 2\|\eta\|_2) \end{aligned}$$

Therefore, recalling that  $x^\perp := x_0 - \Pi_{\mathcal{R}(G)} x_0$ ,

$$\begin{aligned} \|\hat{x} - x_0\|_2 &\leq \|x_* - x_0\|_2 + \|\hat{x} - x_*\|_2 \\ &\leq \|x_* - x_0\|_2 + \frac{1}{1 - \delta} (2\|A(x_* - x_0)\|_2 + \varepsilon + 2\|\eta\|_2) \\ &\leq \frac{5 + 3\delta}{1 - \delta} \|x_* - x_0\|_2 + \frac{1}{1 - \delta} (2\|Ax^\perp\|_2 + 2\|\eta\|_2 + \varepsilon). \end{aligned}$$

In the final inequality, we have used that

$$\|A(x_* - x_0)\|_2 \leq (1 + \delta)\|x_* - \Pi_{\mathcal{R}(G)} x_0\|_2 + \|Ax^\perp\|_2$$

together with the fact that  $\|x_* - \Pi_{\mathcal{R}(G)} x_0\|_2 \leq 2\|x_* - x_0\|_2$ .  $\square$

*Proof of Lemma II.4.* Observe that  $I = \sum_{i=1}^n U_i U_i^*$  since  $U$  is a unitary matrix. Thus, since  $\Pi_{\mathcal{L}}^2 = \Pi_{\mathcal{L}}$ ,

$$\begin{aligned} &\sup_{x \in \mathcal{L} \cap \mathbb{S}^{n-1}} \|\|Ax\|_2^2 - 1\| \\ &= \sup_{x \in \mathcal{L} \cap \mathbb{S}^{n-1}} |x^\top (A^* A - I)x| \\ &= \sup_{x \in \mathcal{L} \cap \mathbb{S}^{n-1}} \left| x^\top \Pi_{\mathcal{L}}^\top \left( \frac{n}{m} \sum_{i=1}^n \theta_i U_i U_i^* - \sum_{i=1}^n U_i U_i^* \right) \Pi_{\mathcal{L}} x \right|. \end{aligned}$$

Define  $\tilde{U}_i := \Pi_{\mathcal{L}} U_i = \Pi_{\mathcal{L}}^\top U_i$ , using that  $\Pi_{\mathcal{L}}$  is an orthogonal projection, hence symmetric. Then,

$$\begin{aligned} &\sup_{x \in \mathcal{L} \cap \mathbb{S}^{n-1}} \|\|Ax\|_2^2 - 1\| \\ &= \sup_{x \in \mathcal{L} \cap \mathbb{S}^{n-1}} \left| x^\top \frac{n}{m} \left( \sum_{i=1}^n \left( \theta_i - \frac{m}{n} \right) \tilde{U}_i \tilde{U}_i^* \right) x \right|. \end{aligned}$$

Since  $x$  and  $\tilde{U}_i$  belong to a  $k$ -dimensional subspace, there exists an isometry so that we may view  $\tilde{U}_i$  as a  $k$ -dimensional vector. By abuse of notation, for  $\tilde{U}_i \in \mathbb{C}^k$  and  $\|\cdot\|_{\text{op}}$  being the operator norm for a Hermitian matrix over  $\mathbb{R}^k$  induced by the Euclidean norm,

$$\sup_{x \in \mathcal{L} \cap \mathbb{S}^{n-1}} \|\|Ax\|_2^2 - 1\| = \left\| \frac{n}{m} \sum_{i=1}^n \left( \theta_i - \frac{m}{n} \right) \tilde{U}_i \tilde{U}_i^* \right\|_{\text{op}}.$$

We will apply the matrix Bernstein inequality ([Lemma A.1](#)) to achieve concentration of the operator norm of the sum of mean-zero random matrices above. By the  $\alpha$ -coherence assumption,  $\|\tilde{U}_i\|_2^2 = \sup_{x \in \mathcal{L} \cap \mathbb{S}^{n-1}} |\langle x, U_i \rangle|^2 \leq \alpha^2$ . Consequently, the operator norm of each constituent matrix is bounded almost surely: for each  $i \in [n]$ ,

$$\left\| \frac{n}{m} \tilde{U}_i \tilde{U}_i^* \left( \theta_i - \frac{m}{n} \right) \right\|_{\text{op}} \leq \frac{n}{m} \|\tilde{U}_i \tilde{U}_i^*\|_{\text{op}} = \frac{n}{m} \|\tilde{U}_i\|_2^2 \leq \frac{n}{m} \alpha^2$$

and the operator norm of the covariance matrix is bounded as

$$\begin{aligned} &\left\| \frac{n^2}{m^2} \sum_{i=1}^n \|\tilde{U}_i\|_2^2 \tilde{U}_i \tilde{U}_i^* \mathbb{E} \left( \theta_i - \frac{m}{n} \right)^2 \right\|_{\text{op}} \\ &= \left\| \frac{n^2}{m^2} \sum_{i=1}^n \|\tilde{U}_i\|_2^2 \tilde{U}_i \tilde{U}_i^* \frac{m}{n} \left( 1 - \frac{m}{n} \right) \right\|_{\text{op}} \leq \alpha^2 \left( \frac{n}{m} - 1 \right). \end{aligned}$$

Therefore, by [Lemma A.1](#) it follows that

$$\begin{aligned} &\mathbb{P} \left\{ \left\| \frac{n}{m} \sum_{i=1}^n \tilde{U}_i \tilde{U}_i^* \left( \theta_i - \frac{m}{n} \right) \right\|_{\text{op}} \geq \delta \right\} \\ &\leq 2k \exp \left( - \frac{m\delta^2/2}{n\alpha^2 \left( 1 - \frac{m}{n} + \frac{\delta}{3} \right)} \right) \\ &\leq 2k \exp \left( -C \cdot \min \left\{ \frac{m\delta^2}{n\alpha^2(1 - m/n)}, \frac{m\delta}{n\alpha^2} \right\} \right). \end{aligned}$$

To complete the proof, we adapt the argument from the proof of ([Vershynin, 2018](#), Theorem 3.1.1). Indeed, for  $\delta \geq 0$  note that  $|1 - z| > \delta \implies |z^2 - 1| > \max(\delta, \delta^2)$  yields the implication  $\max_i |1 - z_i| > \delta \implies \max_i |z_i^2 - 1| > \max(\delta, \delta^2)$ . Consequently,

$$\begin{aligned} &\mathbb{P} \left\{ \sup_{x \in \mathcal{L} \cap \mathbb{S}^{n-1}} |\|Ax\|_2 - 1| \geq \delta \right\} \\ &\leq \mathbb{P} \left\{ \sup_{x \in \mathcal{L} \cap \mathbb{S}^{n-1}} |\|Ax\|_2^2 - 1| \geq \max(\delta, \delta^2) \right\} \\ &\leq 2k \exp \left( - \frac{C\delta^2 m}{\alpha^2 n} \right). \end{aligned}$$

$\square$

## B. Proofs for Typical Coherence

The proof of [Proposition III.1](#) requires the following lemma.

**Lemma V.1.** Let  $A \in \mathbb{C}^{n \times k}$  be a matrix with  $\ell_2$ -normalized columns and let  $A_i$  denote the  $i$ th row of  $A$ . Then

$$\max_{i \in [n]} \|A_i\|_2 \geq \sqrt{\frac{k}{n}}.$$

We now prove the theorem using the lemma.

*Proof of Proposition III.1.* Take the set  $\mathcal{T}$  of all subspaces of dimension  $k$  in  $\mathbb{C}^n$ . By rotational invariance of  $\mathcal{T}$ , it suffices to show the result with respect to  $U = I$ . Hence, let  $\{e_i\}_{i \in [n]}$  be the canonical basis. Any fixed  $T \in \mathcal{T}$  has coherence

$$\alpha = \sup_{v \in T \cap \mathbb{S}^{n-1}} \|v\|_\infty.$$

We will show a sharp lower bound on the coherence of all  $k$ -dimensional subspaces, namely

$$\inf_{T \in \mathcal{T}} \sup_{v \in T \cap \mathbb{S}^{n-1}} \|v\|_\infty = \sqrt{\frac{k}{n}}.$$

Take the set  $\mathcal{A} \subseteq \mathbb{C}^{n \times k}$  of orthonormal matrices. Since  $\mathcal{T} = \{\mathcal{R}(A) : A \in \mathcal{A}\}$ , it follows that

$$\begin{aligned} \inf_{T \in \mathcal{T}} \sup_{v \in T \cap \mathbb{S}^{n-1}} \|v\|_\infty &= \inf_{A \in \mathcal{A}} \sup_{\nu \in \mathbb{S}^{k-1}} \|A\nu\|_\infty \\ &= \inf_{A \in \mathcal{A}} \max_{i \in [n]} \sup_{\nu \in \mathbb{S}^{k-1}} |A_i \nu| \\ &= \inf_{A \in \mathcal{A}} \max_{i \in [n]} \|A_i\|_2. \end{aligned}$$

Apply [Lemma V.1](#) to lower bound the latter quantity. As [Lemma V.1](#) applies to any matrix in  $\mathcal{A}$ ,

$$\inf_{A \in \mathcal{A}} \sup_{i \in [n]} \|A_i\|_2 \geq \sqrt{\frac{k}{n}}.$$

We next show equality. Take  $F \in \mathbb{C}^{n \times k}$  whose columns are the first  $k$  columns of the DFT matrix, as defined in [Remark I.1](#). The columns of  $F$  are orthonormal, so  $F \in \mathcal{A}$ . Furthermore, each row of  $F$  has  $\ell_2$  norm  $\sqrt{\frac{k}{n}}$ . It follows that

$$\inf_{A \in \mathcal{A}} \max_{i \in [n]} \|A_i\|_2 = \sqrt{\frac{k}{n}}.$$

□

*Proof of Lemma V.1.* Computing directly, using that each of the  $k$  columns has unit norm,

$$\max_{i \in [n]} \|A_i\|_2^2 \geq \text{mean}_{i \in [n]} \|A_i\|_2^2 = \frac{1}{n} \|A\|_F^2 = \frac{k}{n}.$$

Taking square roots completes the proof. □

The proof of [Theorem III.2](#) uses [Lemma A.2](#) and the following lemma, which bounds the coherence of a random subspace sampled from the *Grassmannian*. The Grassmannian  $\Gamma_{n,k}$  consists of all  $k$ -dimensional subspaces of  $\mathbb{R}^n$  ([Vershynin, 2018](#), Ch. 5.2.6).

**Lemma V.2.** *Let  $U \in \mathbb{C}^{n \times n}$  be a unitary matrix and denote by  $\mathcal{L} \in \Gamma_{n,k}$  a subspace distributed uniformly at random over  $\Gamma_{n,k}$ . With probability at least  $1 - 2 \exp(-\gamma^2)$ ,  $\mathcal{L}$  is  $\alpha$ -coherent with respect to  $\|\cdot\|_U$  with*

$$\alpha \lesssim \sqrt{\frac{k}{n}} + \sqrt{\frac{\log(n)}{n}} + \frac{\gamma}{\sqrt{n}}.$$

*Proof of Theorem III.2.* By [Lemma A.4](#),  $\mathcal{R}(G)$  is contained in the union of  $N$  at-most  $k$ -dimensional subspaces with

$$\log N \leq k \sum_{i=1}^{d-1} \log \left( \frac{2ek_i}{k} \right).$$

Each subspace is uniformly distributed on  $\Gamma_{n,k}$  because the final weight matrix has iid Gaussian entries independent of the other weight matrices (e.g., see [Vershynin \(2018, Ch. 3.3.2\)](#)). It follows that  $\mathcal{R}(G) - \mathcal{R}(G)$  is contained in  $M = (1/2)(N^2 + N) \leq N^2$  subspaces each of dimension at-most  $2k$ . Applying [Lemma V.2](#), we see that the coherence of each subspace is a random variable  $\alpha_i$  such that

$$\alpha_i \lesssim \sqrt{\frac{k}{n}} + \sqrt{\frac{\log(n)}{n}} + \frac{\gamma}{\sqrt{n}}$$

with probability at least  $1 - 2 \exp(-\gamma^2)$ .

Let  $\alpha$  be the coherence of  $\mathcal{R}(G) - \mathcal{R}(G)$  and observe that  $\alpha \leq \max_{i \in [M]} \alpha_i$ . Applying [Lemma A.2](#),

$$\alpha \leq \max_{i \in [M]} (\alpha_i) \lesssim \sqrt{\frac{k}{n}} + \sqrt{\frac{\log(n)}{n}} + \sqrt{\frac{\log M}{n}} + \frac{\gamma}{\sqrt{n}}$$

with probability at least  $1 - 2 \exp(-\gamma^2)$ .

Since  $\log M \lesssim \log N$ , the statement follows. □

We next prove [Lemma V.2](#).

*Proof of Lemma V.2.* Let  $A \in \mathbb{R}^{n \times k}$  with  $A_{ij} \stackrel{\text{iid}}{\sim} \mathcal{N}(0, 1)$ . Then,  $\mathcal{L} := \mathcal{R}(A)$  is a random subspace uniformly distributed over  $\Gamma_{n,k}$ . By rotation invariance of the Grassmannian, it suffices to show the result for  $U = I$ . Let  $\{e_i\}_{i \in [n]}$  denote the canonical basis. Define

$$\alpha := \sup_{v \in \mathcal{L} \cap \mathbb{S}^{n-1}} \max_{i \in [n]} |\langle e_i, v \rangle|,$$

and note that  $\mathcal{L}$  is  $\alpha$ -coherent with respect to  $\|\cdot\|_I = \|\cdot\|_\infty$ . For each  $i \in [n]$ , we next analyze

$$\alpha_i := \sup_{v \in \mathcal{L} \cap \mathbb{S}^{n-1}} |\langle e_i, v \rangle| = \sup_{y \in \mathbb{S}^{k-1}} \left| \frac{A_i y}{\|A y\|_2} \right| \quad (4)$$

We will show, with probability at least  $1 - 4 \exp(-s^2)$ ,

$$\alpha_i \lesssim \sqrt{\frac{k}{n}} + \frac{s}{\sqrt{n}}.$$

To see why this result should hold, we focus our attention on the right hand side of (4). The denominator concentrates around  $\sqrt{n}$  and the numerator is bounded by  $\|A_i\|_2$ , which concentrates around  $\sqrt{k}$  with subgaussian tails.

We first obtain a lower bound on the smallest singular value of  $A$  via ([Vershynin, 2018](#), Theorem 4.6.1), which guarantees with probability at least  $1 - 2 \exp(-t^2)$  that

$$\inf_{y \in \mathbb{S}^{k-1}} \|A y\|_2 \geq \sqrt{n} - C\sqrt{k} - Ct.$$

By fixing  $t = \frac{\sqrt{n}}{2C}$  we define the event

$$B := \left\{ \inf_{y \in \mathbb{S}^{k-1}} \|A y\|_2 \leq \frac{\sqrt{n}}{2} - C\sqrt{k} \right\}$$

$$\begin{aligned} &\mathbb{P} \left\{ \sup_{y \in \mathbb{S}^{k-1}} \frac{A_i y}{\|A y\|_2} > \frac{\sqrt{k} + s}{\frac{\sqrt{n}}{2} - C\sqrt{k}} \right\} \\ &= \mathbb{P} \left\{ \sup_{y \in \mathbb{S}^{k-1}} \frac{A_i y}{\|A y\|_2} > \frac{\sqrt{k} + s}{\frac{\sqrt{n}}{2} - C\sqrt{k}} \middle| B \right\} \mathbb{P} \{B\} \\ &+ \mathbb{P} \left\{ \sup_{y \in \mathbb{S}^{k-1}} \frac{A_i y}{\|A y\|_2} > \frac{\sqrt{k} + s}{\frac{\sqrt{n}}{2} - C\sqrt{k}} \middle| B^c \right\} \mathbb{P} \{B^c\} \\ &\leq \mathbb{P} \{B\} + \mathbb{P} \left\{ \sup_{y \in \mathbb{S}^{k-1}} A_i y > \sqrt{k} + s \right\} \\ &\leq 2 \exp(-cn) + \mathbb{P} \left\{ \|A_i\|_2 > \sqrt{k} + s \right\} \\ &\leq 2 \exp(-cn) + 2 \exp(-cs^2). \end{aligned}$$

Above, we used the concentration of the norm of Gaussian vectors (Vershynin, 2018, Theorem 3.1.1). Since  $s \leq C\sqrt{n}$ ,  $\exp(-cn) \leq \exp(-cs^2)$ . From this we find the desired subgaussian tail bound;

$$\mathbb{P} \left\{ \sup_{y \in \mathbb{S}^{k-1}} \frac{A_i y}{\|A y\|_2} > \frac{\sqrt{k} + s}{\frac{\sqrt{n}}{2} - C\sqrt{k}} \right\} \leq 4 \exp(-cs^2).$$

The remaining values of  $s$  satisfy  $\sqrt{k} + s > \frac{\sqrt{n}}{2} - C\sqrt{k}$ . Therefore, since  $\sup_{y \in \mathbb{S}^{k-1}} \frac{A_i y}{\|A y\|_2} \leq 1$ ,

$$\mathbb{P} \left\{ \sup_{y \in \mathbb{S}^{k-1}} \frac{A_i y}{\|A y\|_2} > \frac{\sqrt{k} + s}{\frac{\sqrt{n}}{2} - C\sqrt{k}} \right\} = 0 \leq 4 \exp(-cs^2).$$

Therefore, the subgaussian bound applies for all values of  $s$ .

We now scale  $s$  by an absolute constant with  $\gamma = cs$ . Then

$$\alpha_i = \sup_{y \in \mathbb{S}^{k-1}} \left| \frac{A_i y}{\|A y\|_2} \right| > \frac{\sqrt{k} + s}{\frac{\sqrt{n}}{2} - C\sqrt{k}} \gtrsim \sqrt{\frac{k}{n}} + \frac{\gamma}{\sqrt{n}}$$

with probability less than  $2 \exp(-\gamma^2)$ . Changing the constant from 4 to 2 in the probability bound is achieved by suitable choice of  $c$ . Remembering that  $\alpha$  is the coherence with the canonical basis, we apply [Lemma A.2](#) to find,

$$\alpha = \max_{i \in [n]} \alpha_i \lesssim \sqrt{\frac{k}{n}} + \sqrt{\frac{\log n}{n}} + \frac{\gamma}{\sqrt{n}}$$

with probability at least  $1 - 2 \exp(-\gamma^2)$ .  $\square$

## VI. CONCLUSION

In this work, we have proved a restricted isometry property for a subsampled isometry with GNN structural proxy, [Theorem II.2](#). We used this to prove sample complexity and recovery bounds, [Theorem II.1](#). The recovery bound stated in [Theorem II.1](#) is uniform over ground truth signals, and permits a more finely tuned non-uniform control as discussed in [Remark II.1](#). To our knowledge, this provides the first theory for generative compressed sensing with subsampled isometries and non-random weights, albeit with a sample complexity that is off by a factor of  $k$  compared to the best subgaussian theory (Bora et al., 2017).

Our results rely on the notion of  $\alpha$ -coherence with respect to the measurement norm, introduced in [Definition I.4](#) and [Definition I.3](#), respectively. Closely related to the notion of incoherent bases (Foucart and Rauhut, 2013, p. 373) and the  $X$ -norm of Rudelson and Vershynin (2008), we argue that  $\alpha$ -coherence is a natural quantity to measure the interplay between a GNN and the measurement operator. Indeed, in [§ IV](#) we propose a regularization strategy for promoting favourable coherence of GNNs during training, and connect this strategy with favourable recovery efficacy. Specifically, we show that our regularization strategy yields low coherence GNNs with improved sample complexity for recovery ([Figure 3](#)). Moreover, our numerics support that low coherence GNNs achieve better sample complexity than high coherence GNNs ([Figure 1](#)).

We believe the sample complexity of our analysis has sub-optimal dependence on  $k$ , namely  $\Omega(k^2)$ , which may be a

consequence of our coherence-based approach. It is an open question to remove this extra factor of  $k$ . In addition, it is an open problem to improve the regularization strategy for lowering coherence, possibly including middle layers. Finally, it is open to determine a notion of coherence for networks that have a final nonlinear activation function, and to characterize how this impacts recovery efficacy for such networks.

## REFERENCES

Ben Adcock and Anders C Hansen. *Compressive Imaging: Structure, Sampling, Learning*. Cambridge University Press, Cambridge, UK, 2021.

Ben Adcock, Simone Brugiapaglia, and Clayton G Webster. *Sparse Polynomial Approximation of High-Dimensional Functions*. SIAM, Philadelphia, PA, 2022.

Aaron Berk. Deep generative demixing: Error bounds for demixing subgaussian mixtures of Lipschitz signals. In *ICASSP 2021-2021 IEEE International Conference on Acoustics, Speech and Signal Processing (ICASSP)*, pages 4010–4014. IEEE, 2021.

Aaron Berk, Simone Brugiapaglia, Babhru Joshi, Yaniv Plan, Matthew Scott, and Özgür Yilmaz. subIso GCS. *GitHub repository*, 2022. <https://github.com/babhrujoshi/GNN-with-sub-Fourier-paper>.

Ashish Bora, Ajil Jalal, Eric Price, and Alexandros G Dimakis. Compressed sensing using generative models. In *International Conference on Machine Learning*, pages 537–546, 2017.

Stéphane Boucheron, Gábor Lugosi, and Pascal Massart. *Concentration Inequalities: A Nonasymptotic Theory of Independence*. Oxford University Press, Oxford, UK, 2013.

Jean Bourgain. An improved estimate in the restricted isometry problem. In *Geometric aspects of functional analysis*, pages 65–70. Springer, 2014.

Simone Brugiapaglia, Sjoerd Dirksen, Hans Christian Jung, and Holger Rauhut. Sparse recovery in bounded Riesz systems with applications to numerical methods for PDEs. *Applied and Computational Harmonic Analysis*, 53:231–269, 2021.

Emmanuel J Candès and Justin Romberg. Sparsity and incoherence in compressive sampling. *Inverse problems*, 23(3):969, 2007.

Emmanuel J Candès, Justin Romberg, and Terence Tao. Robust uncertainty principles: Exact signal reconstruction from highly incomplete frequency information. *IEEE Transactions on information theory*, 52(2):489–509, 2006.

Joshua Cape, Minh Tang, and Carey E Priebe. The two-to-infinity norm and singular subspace geometry with applications to high-dimensional statistics. *The Annals of Statistics*, 47(5):2405–2439, 2019.

Abdellah Chkifa, Nick Dexter, Hoang Tran, and Clayton G Webster. Polynomial approximation via compressed sensing of high-dimensional functions on lower sets. *Mathematics of Computation*, 87(311):1415–1450, 2018.

Thomas M Cover. Geometrical and statistical properties of systems of linear inequalities with applications in pattern recognition. *IEEE Transactions on Electronic Computers*, EC-14(3):326–334, 1965. doi: 10.1109/PGEC.1965.264137.

Mohammad Zalbagi Darestani and Reinhard Heckel. Accelerated MRI with un-trained neural networks. *IEEE Transactions on Computational Imaging*, 7:724–733, 2021.

Li Deng. The MNIST database of handwritten digit images for machine learning research. *IEEE Signal Processing Magazine*, 29(6):141–142, 2012.

Puneesh Deora, Bhavya Vasudeva, Saumik Bhattacharya, and Pyari Mohan Pradhan. Structure preserving compressive sensing MRI reconstruction using generative adversarial networks. In *Proceedings of the IEEE/CVF Conference on Computer Vision and Pattern Recognition Workshops*, pages 522–523, 2020.

Sjoerd Dirksen. Tail bounds via generic chaining. *Electronic Journal of Probability*, 20, 2015.

David L Donoho. Compressed sensing. *IEEE Transactions on information theory*, 52(4):1289–1306, 2006.

David L Donoho and Michael Elad. Optimally sparse representation in general (nonorthogonal) dictionaries via  $\ell_1$  minimization. *Proceedings of the National Academy of Sciences*, 100(5):2197–2202, 2003.

Leopold Flatto. A new proof of the transposition theorem. *Proceedings of the American Mathematical Society*, 24(1):29–31, 1970.

Simon Foucart and Holger Rauhut. *A Mathematical Introduction to Compressive Sensing*. Applied and Numerical Harmonic Analysis. Birkhäuser, New York, NY, 2013.

Ian Goodfellow, Jean Pouget-Abadie, Mehdi Mirza, Bing Xu, David Warde-Farley, Sherjil Ozair, Aaron Courville, and Yoshua Bengio. Generative adversarial nets. In *Advances in Neural Information Processing Systems*, pages 2672–2680, 2014.

Paul Hand and Babbu Joshi. Global guarantees for blind demodulation with generative priors. In *Advances in Neural Information Processing Systems*, volume 32, pages 11535–11545, 2019.

Paul Hand and Vladislav Voroninski. Global guarantees for enforcing deep generative priors by empirical risk. *IEEE Transactions on Information Theory*, 66(1):401–418, 2019.

Paul Hand, Oscar Leong, and Vladislav Voroninski. Phase retrieval under a generative prior. *Advances in Neural Information Processing Systems*, 31, 2018.

Ishay Haviv and Oded Regev. The restricted isometry property of subsampled Fourier matrices. In *Geometric aspects of functional analysis*, pages 163–179. Springer, 2017.

Reinhard Heckel and Paul Hand. Deep Decoder: Concise image representations from untrained non-convolutional networks. In *International Conference on Learning Representations*, 2019.

Felix J Herrmann, Michael P Friedlander, and Özgür Yilmaz. Fighting the curse of dimensionality: Compressive sensing in exploration seismology. *IEEE Signal Processing Magazine*, 29(3):88–100, 2012.

Mike Innes. Flux: Elegant machine learning with julia. *Journal of Open Source Software*, 3(25):602, 2018.

Laurent Jacques, Jason N Laska, Petros T Boufounos, and Richard G Baraniuk. Robust 1-bit compressive sensing via binary stable embeddings of sparse vectors. *IEEE Transactions on Information Theory*, 59(4):2082–2102, 2013.

Ajil Jalal, Marius Arvinte, Giannis Daras, Eric Price, Alexandros G Dimakis, and Jonathan I Tamir. Robust compressed sensing MRI with deep generative priors. *arXiv preprint arXiv:2108.01368*, 2021.

Halyun Jeong, Xiaowei Li, Yaniv Plan, and Özgür Yilmaz. Sub-gaussian matrices on sets: Optimal tail dependence and applications. *arXiv preprint arXiv:2001.10631*, 2020.

Babbu Joshi, Xiaowei Li, Yaniv Plan, and Özgür Yilmaz. PLUGIn: A simple algorithm for inverting generative models with recovery guarantees. *Advances in Neural Information Processing Systems*, 34, 202book1.

Diederik P Kingma and Jimmy Ba. Adam: A method for stochastic optimization. *arXiv preprint arXiv:1412.6980*, 2014.

Diederik P Kingma and Max Welling. Auto-encoding variational Bayes. *arXiv preprint arXiv:1312.6114*, 2013.

Diederik P Kingma and Max Welling. An introduction to variational autoencoders. *Foundations and Trends in Machine Learning*, 12(4):307–392, 2019.

Rajiv Kumar, Haneet Wason, and Felix J Herrmann. Source separation for simultaneous towed-streamer marine acquisition - a compressed sensing approach. *Geophysics*, 80(6):WD73–WD88, 2015.

Wenzong Li, Aichun Zhu, Yonggang Xu, Hongsheng Yin, and Gang Hua. A fast multi-scale generative adversarial network for image compressed sensing. *Entropy*, 24(6):775, 2022.

Christopher Liaw, Abbas Mehrabian, Yaniv Plan, and Roman Vershynin. A simple tool for bounding the deviation of random matrices on geometric sets. In *Geometric aspects of functional analysis*, pages 277–299. Springer, 2017.

Jiulong Liu and Zhaoqiang Liu. Non-iterative recovery from nonlinear observations using generative models. *arXiv preprint arXiv:2205.15749*, 2022.

Michael Lustig, David L Donoho, Juan M Santos, and John M Pauly. Compressed sensing mri. *IEEE signal processing magazine*, 25(2):72–82, 2008.

Morteza Mardani, Enhao Gong, Joseph Y Cheng, Shreyas S Vasanawala, Greg Zaharchuk, Lei Xing, and John M Pauly. Deep generative adversarial neural networks for compressive sensing MRI. *IEEE transactions on medical imaging*, 38(1):167–179, 2018.

Alireza Naderi and Yaniv Plan. Beyond independent measurements: General compressed sensing with GNN application. *arXiv preprint arXiv:2111.00327*, 2021.

Alireza Naderi and Yaniv Plan. Sparsity-free compressed sensing with generative priors as special case, 2022. Unpublished manuscript.

Roman Novak, Yasaman Bahri, Daniel A Abolafia, Jeffrey Pennington, and Jascha Sohl-Dickstein. Sensitivity and generalization in neural networks: An empirical study. *arXiv preprint arXiv:1802.08760*, 2018.

Alec Radford, Luke Metz, and Soumith Chintala. Unsupervised representation learning with deep convolutional generative adversarial networks. *arXiv preprint arXiv:1511.06434*, 2015.

Holger Rauhut. Compressive sensing and structured random matrices. In *Theoretical foundations and numerical methods for sparse recovery*, pages 1–92. de Gruyter, 2010.

Mark Rudelson and Roman Vershynin. On sparse reconstruction from Fourier and Gaussian measurements. *Communications on Pure and Applied Mathematics: A Journal Issued by the Courant Institute of Mathematical Sciences*, 61(8):1025–1045, 2008.

Jonathan Scarlett, Reinhard Heckel, Miguel RD Rodrigues, Paul Hand, and Yonina C Eldar. Theoretical perspectives on deep learning methods in inverse problems. *arXiv preprint arXiv:2206.14373*, 2022.

Thiago Serra, Christian Tjandraatmadja, and Srikumar Ramalingam. Bounding and counting linear regions of deep neural networks. In *International Conference on Machine Learning*, pages 4558–4566. PMLR, 2018.

Joel A Tropp. User-friendly tail bounds for sums of random matrices. *Foundations of Computational Mathematics*, 12(4):389–434, 2012.

Dmitry Ulyanov, Andrea Vedaldi, and Victor Lempitsky. Deep image prior. In *Proceedings of the IEEE conference on computer vision and pattern recognition*, pages 9446–9454, 2018.

Roman Vershynin. *High-dimensional Probability: An Introduction with Applications in Data Science*. Cambridge University Press, Cambridge, UK, 2018.

Pauli Virtanen, Ralf Gommers, Travis E Oliphant, Matt Haberland, Tyler Reddy, David Cournapeau, Evgeni Burovski, Pearu Peterson, Warren Weckesser, Jonathan Bright, Stéfan J van der Walt, Matthew Brett, Joshua Wilson, K Jarrod Millman, Nikolay Mayorov, Andrew R J Nelson, Eric Jones, Robert Kern, Eric Larson, C J Carey, İlhan Polat, Yu Feng, Eric W Moore, Jake VanderPlas, Denis Laxalde, Josef Perktold, Robert Cimrman, Ian Henriksen, E A Quintero, Charles R Harris, Anne M Archibald, Antônio H Ribeiro, Fabian Pedregosa, Paul van Mulbregt, and SciPy 1.0 Contributors. SciPy 1.0: Fundamental algorithms for scientific computing in Python. *Nature Methods*, 17(3):261–272, 2020.

Jacqueline Wentz and Alireza Doostan. GenMod: A generative modeling approach for spectral representation of PDEs with random inputs. *arXiv preprint arXiv:2201.12973*, 2022.

## APPENDIX

### A. Results from high-dimensional probability

1) *Matrix Bernstein inequality*: For this result, see [Tropp \(2012, Theorem 6.1\)](#).

**Lemma A.1** (Matrix Bernstein inequality). *Let  $X_1, \dots, X_N \in \mathbb{C}^{n \times n}$  be independent, mean-zero, self-adjoint random matrices, such that  $\|X_i\| \leq K$  almost surely for all  $i$ . Then, for every  $\gamma \geq 0$  we have*

$$\begin{aligned} \mathbb{P} \left\{ \left\| \sum_{i=1}^N X_i \right\| \geq \gamma \right\} &\leq 2n \exp \left( -\frac{\gamma^2/2}{\sigma^2 + K\gamma/3} \right) \\ &\leq 2n \exp \left( -c \cdot \min \left( \frac{\gamma^2}{\sigma^2}, \frac{\gamma}{K} \right) \right). \end{aligned}$$

Here,  $\sigma^2 := \left\| \sum_{i=1}^N \mathbb{E} X_i^2 \right\|$ .

2) *Cramér-Chernoff bound*: For a reference to this material, see [Boucheron et al. \(2013, Ch. 2.2\)](#). Let  $Z$  be a real-valued random variable. Then,

$$\mathbb{P} \{Z \geq t\} \leq \exp(-\psi_Z^*(t)), \quad \psi_Z^*(t) := \sup_{\lambda \geq 0} \lambda t - \psi_Z(\lambda).$$

The latter quantity,  $\psi_Z^*(t)$ , is the Cramér transform of  $Z$ , with

$$\psi_Z(\lambda) := \log \mathbb{E} \exp(\lambda Z), \quad \lambda \geq 0$$

being the logarithm of the moment generating function of  $Z$ . When  $Z$  is centered,  $\psi_Z$  is continuously differentiable on an interval of the form  $[0, b)$  and  $\psi_Z(0) = \psi'_Z(0) = 0$ . Thus,

$$\psi_Z^*(t) = \lambda_t t - \psi_Z(\lambda_t),$$

where  $\lambda_t$  is such that  $\psi'_Z(\lambda_t) = t$ .

For a centered binomial random variable  $Z := Y - np$  where  $Y \sim \text{Binom}(n, p)$ , the Cramér transform of  $Z$  is given by

$$\psi_Z^*(t) := nh_p \left( \frac{t}{n} + p \right), \quad \forall 0 < t < n(1-p),$$

where  $h_p(a) := (1-a) \log \frac{1-a}{1-p} + a \log \frac{a}{p}$  is the Kullback-Leibler divergence  $D_{\text{KL}}(P_a \parallel P_p)$  between Bernoulli distributions with parameters  $a$  and  $p$ . One may thus establish [\(Boucheron et al., 2013, Ch. 2.2\)](#) the following concentration inequality for  $Y$  when  $0 < t < \frac{n}{m}$ :

$$\mathbb{P} \{Y \geq tm\} = \mathbb{P} \{Z \geq (t-1)m\} \leq \exp(-nh_p(tp)).$$

### 3) Auxiliary union bound:

**Lemma A.2.** *Let  $f : \mathbb{R} \rightarrow \mathbb{R}$  be an increasing function. Let  $\{X_i\}_{i \in [n]}$  be a collection of random variables such that for each  $i \in [n]$  and for any  $\gamma > 0$ ,*

$$X_i \leq f(\gamma)$$

*with probability at least  $1 - 2 \exp(-\gamma^2)$ . Then, for all  $\gamma > 0$ ,*

$$\max_{i \in [n]} X_i \leq f \left( c \left( \gamma + \sqrt{\log n} \right) \right)$$

*with probability at least  $1 - 2 \exp(-\gamma^2)$ .*

*Proof of Lemma A.2.* By assumption,

$$\begin{aligned} \mathbb{P} \left\{ \max_{i \in [n]} X_i > f(\gamma) \right\} &= \mathbb{P} \left\{ \bigcup_{i \in [n]} \{X_i > f(\gamma)\} \right\} \\ &\leq n 2 \exp(-\gamma^2) \\ &= 2 \exp(-\gamma^2 + \log n). \end{aligned}$$

Let  $t := \sqrt{\gamma^2 - \log n}$ . We substitute  $\gamma^2 \rightarrow t^2 + \log n$  in the right hand side of the equation above which yields

$$\mathbb{P} \left\{ \max_{i \in [n]} X_i > f(\gamma) \right\} \leq 2 \exp(-t^2).$$

To substitute the remaining  $\gamma$  on the left hand side, first notice

$$\gamma \leq 2 \max(t, \sqrt{\log n}) \leq 2 \left( t + \sqrt{\log n} \right).$$

Consequently,  $f(\gamma) \leq f(2(t + \sqrt{\log n}))$  and

$$\begin{aligned} \mathbb{P} \left\{ \max_{i \in [n]} X_i > f \left( 2 \left( t + \sqrt{\log n} \right) \right) \right\} &\leq \mathbb{P} \left\{ \max_{i \in [n]} X_i > f(\gamma) \right\} \\ &\leq 2 \exp(-t^2) \end{aligned}$$

Re-labelling  $t \rightarrow \gamma$  yields the result.  $\square$

### B. Characterizing $\mathcal{R}(G)$

For completeness, we include a characterization of the geometry of the range of generative neural networks with ReLU activation. This material is not novel; for instance, see [Naderi and Plan \(2021\)](#). It requires the notion of a low-dimensional cone.

**Definition A.1.** A convex set  $\mathcal{C} \subseteq \mathbb{R}^n$  is *at-most  $k$ -dimensional* for some  $k \in [n]$  if there exists a linear subspace  $E \subseteq \mathbb{R}^n$  with  $\dim(E) \leq k$  and  $\mathcal{C} \subseteq E$ .

**Remark A.1.** A cone  $\mathcal{C} \subseteq \mathbb{R}^n$  is at-most  $k$ -dimensional if its linear hull,  $\text{span}(\mathcal{C})$ , is no greater than  $k$ -dimensional.  $\diamond$

A key idea in our recovery guarantees will be to cover  $\mathcal{R}(G)$  using at-most  $k$ -dimensional cones. To this end, it will be important to bound the number  $N$  of at-most  $k$ -dimensional cones in the covering set. This comes down to quantifying the number of different ways that ReLU can act on a given subspace, which reduces to counting the number of orthants that subspace intersects. The following result may be found in [Jacques et al. \(2013, App. A Lemma 1\)](#).

**Lemma A.3** (orthant-crossings). *Let  $S \subseteq \mathbb{R}^n$  be a  $k$ -dimensional subspace. Then  $S$  intersects at most  $I(n, k)$  different orthants where*

$$I(n, k) \leq 2^k \binom{n}{k} \leq 2^k \left(\frac{en}{k}\right)^k. \quad (5)$$

Note that previous work ([Cover, 1965](#); [Flatto, 1970](#)) has established the bound

$$I(n, k) \leq 2 \sum_{\ell=0}^{k-1} \binom{n-1}{\ell},$$

which is tight ([Cover, 1965](#)). Accordingly, the extent of non-tightness of the bound (5) may be evaluated directly for specific choices of  $n$  and  $k$ . The upper bound on  $N$  is an immediate consequence. Note that a version of this result may be found in [Naderi and Plan \(2021\)](#).

**Lemma A.4.** *Let  $G$  be a  $(k, d, n)$ -generative network. Then,  $\mathcal{R}(G)$  is contained in a union of no more than  $N$  at-most  $k$ -dimensional cones where*

$$N := \prod_{\ell=1}^{d-1} I(k_\ell, k) \leq \left(\frac{2e\bar{k}}{k}\right)^{k(d-1)},$$

$$\bar{k} := \left(\prod_{\ell=1}^{d-1} k_\ell\right)^{1/(d-1)}.$$

*Proof of Lemma A.4.* The proof is similar to the one given in [Naderi and Plan \(2021\)](#), repeated here for completeness. Consider that the final mapping  $W^d$  cannot increase the number of cones. Thus, it suffices to consider the map  $\sigma(W^{d-1} \dots \sigma(W^1 u))$ . We need only count the number of new intersected subspaces that could be generated from each ReLU operation. As there are  $d-1$  in total, we obtain

$$\prod_{\ell=1}^{d-1} I(k_\ell, k) \leq 2^{(d-1)k} \prod_{\ell=1}^{d-1} \left(\frac{ek_\ell}{k}\right)^k = \left(\frac{2e\bar{k}}{k}\right)^{k(d-1)},$$

where  $\bar{k}$  is the geometric mean  $\bar{k} := \left(\prod_{\ell=1}^{d-1} k_\ell\right)^{1/(d-1)}$ .  $\square$

**Remark A.2.** A simple calculation shows that

$$\log N \leq k \sum_{i=1}^{d-1} \log \left(\frac{2ek_i}{k}\right).$$

$\diamond$

**Remark A.3.** If  $G$  is a  $d$  layer neural network with ReLU activation then  $G(x) - G(y)$  can be written as  $\bar{G}(x, y) := G(x) - G(y)$  where  $\bar{G} : \mathbb{R}^{2k} \rightarrow \mathbb{R}^n$  is a  $d$ -layer neural network whose  $i$ th weight matrix is

$$\begin{bmatrix} W^{(i)} & \mathbf{0}_{k_i \times k_{i-1}} \\ \mathbf{0}_{k_i \times k_{i-1}} & W^{(i)} \end{bmatrix}$$

for  $i = 1, \dots, d-1$  where  $\mathbf{0}_{m,n}$  is the  $m \times n$  zero matrix. The  $d$ th weight matrix of  $\bar{G}$  is  $\begin{bmatrix} W^{(d)} & -W^{(d)} \end{bmatrix}$ . In particular, the layer widths of  $\bar{G}$  are  $2\bar{k}_0 = 2k, 2k_1, \dots, 2k_{d-1}, k_d = n$ , so applying [Lemma A.4](#) to  $\bar{G}$  gives

$$N(\bar{G}) \leq \left(\frac{2e\bar{k}}{k}\right)^{2k(d-1)}, \quad \log N(\bar{G}) \leq 2k \sum_{i=1}^{d-1} \log \left(\frac{2ek_i}{k}\right),$$

where  $\bar{k}$  is the geometric mean of the layer widths of the original network  $G$ .  $\diamond$

### C. Controlling approximation error

Suppose that  $A \in \mathbb{C}^{m \times n}$  is an  $(m, \theta, U)$ -subsampled isometry with associated unitary matrix  $U \in \mathbb{C}^{n \times n}$ . Recall that  $U^*U = I$  where  $I$  is the identity matrix, and that  $\theta_i \stackrel{\text{iid}}{\sim} \text{Ber}(\frac{m}{n})$ . Let  $x \in \mathbb{C}^n$  be a fixed vector such that  $\|x\|_2 = 1$ . We would like to estimate the tail

$$\mathbb{P}\{\|Ax\|_2^2 \geq t\}$$

for  $t \geq 1$ , so as to imply a high probability bound of the form  $\|Ax\|_2^2 \leq t\|x\|_2^2$  for any fixed  $x \in \mathbb{C}^n$ . For technical reasons yet to be clarified, we also assume  $t < n/m$ .

1) *Reformulation:* Observe that  $A^*A = \frac{n}{m}U^*\text{diag}(\theta)U$ , implying

$$\|Ax\|_2^2 = x^*A^*Ax = \frac{n}{m}x^*U\text{diag}(\theta)Ux = \frac{n}{m} \sum_{i=1}^n \theta_i |z_i|^2,$$

where  $z := Ux$  and  $\|z\|_2 = \|Ux\|_2 = 1$ . Hence, the problem can be recast as bounding the following tail:

$$\mathbb{P}\left\{\frac{n}{m} \sum_{i=1}^n \theta_i |z_i|^2 \geq t\right\},$$

for  $t > 0$  and where  $z \in \mathbb{C}^n$  is a fixed vector with  $\|z\|_2 = 1$ .

2) *Special cases:*

a) *Spike:* Assume that  $z := e_1$  is the first standard basis vector. Then

$$\mathbb{P}\left\{\frac{n}{m} \sum_{i=1}^n \theta_i |z_i|^2 \geq t\right\} = \mathbb{P}\left\{\theta_1 \geq t \frac{m}{n}\right\} = \frac{m}{n} \cdot \mathbb{1}\{t \leq n/m\}$$

for any  $t > 0$ . In particular, one cannot expect good concentration of “spiky” vectors.

b) *Flat vector*: Assume that  $z := \mathbf{1}/\sqrt{n} \in \mathbb{C}^n$  is the scaled all-ones vector. In this case, we have

$$\mathbb{P} \left\{ \frac{n}{m} \sum_{i=1}^n \theta_i |z_i|^2 \geq t \right\} = \mathbb{P} \left\{ \sum_{i=1}^n \theta_i \geq tm \right\}$$

which is the tail of a  $\text{Binom}(n, p)$  random variable where  $p := m/n$ .

We use the Cramér-Chernoff bound (see § A2 and Boucheron et al. (2013, Ch. 2.2)). For a centered binomial random variable  $Z := Y - np$  where  $Y \sim \text{Binom}(n, p)$ , the Cramér transform of  $Z$  is given by

$$\psi_Z^*(t) := nh_p \left( \frac{t}{n} + p \right), \quad \forall 0 < t < n(1-p),$$

where

$$h_p(a) := (1-a) \log \frac{1-a}{1-p} + a \log \frac{a}{p}$$

is the Kullback-Leibler divergence  $D_{\text{KL}}(P_a \parallel P_p)$  between Bernoulli distributions with parameters  $a$  and  $p$ . Thus, as presented in Boucheron et al. (2013, Ch. 2.2),

$$\mathbb{P}\{Y \geq tm\} = \mathbb{P}\{Z \geq (t-1)m\} \leq \exp(-nh_p(tp)) \quad (6)$$

where  $p = m/n$ . Note that  $(t-1)m < n(1-p)$  since  $t < n/m$  as assumed at the very beginning. Now, assuming  $t > 1$ , we compute

$$\begin{aligned} h_p(tp) &= (1-tp) \log \frac{1-tp}{1-p} + tp \log t \\ &= tp \log t - (1-tp) \log \left( 1 + \frac{(t-1)p}{1-tp} \right) \\ &\geq tp \log t - (t-1)p \end{aligned}$$

using that  $\log(1+x) \leq x$ . Simplifying the above expression gives, using  $p = m/n$ ,

$$h_p(tp) \geq \frac{m}{n} (t \log t - t + 1). \quad (7)$$

We remark, as an aside, that this lower bound is nonnegative. Combining (6) and (7) gives

$$\mathbb{P} \left\{ \frac{n}{m} \sum_{i=1}^n \theta_i |z_i|^2 \geq t \right\} \leq \exp(-m(t \log t - t + 1)).$$

The above inequality gives an explicit quantification of how concentration occurs in the case of a perfectly flat vector.

c) *“Flattish” vector*: The inequality extends as follows.

**Proposition A.5.** *Let  $\xi \in \mathbb{C}^n$  be a fixed vector satisfying  $\|\xi\|_2 = 1$  and let  $A \in \mathbb{C}^{\tilde{m} \times n}$  be a subsampled isometry associated to a unitary matrix  $U \in \mathbb{C}^{n \times n}$ . Define  $R := n \cdot \|\xi\|_U^2$ . Then, for all  $1 < t < \frac{n}{m}$ ,*

$$\mathbb{P} \{ |\|A\xi\|_2^2 - 1| \geq t \} \leq \exp \left( -m \left( \frac{t}{R} \log \frac{t}{R} - \frac{t}{R} + 1 \right) \right).$$

The proof of the result follows readily from the discussion above for a *Flat vector*. Assume instead that  $\|z\|_2 = 1$  and  $\|z\|_\infty^2 \leq R/n$ . It is straightforward to show that, for  $t < n/m$ ,

$$\begin{aligned} \mathbb{P} \left\{ \frac{n}{m} \sum_{i=1}^n \theta_i |z_i|^2 \geq t \right\} &\leq \mathbb{P} \left\{ \frac{n}{m} \|z\|_\infty^2 \sum_{i=1}^n \theta_i \geq t \right\} \\ &= \mathbb{P} \left\{ \sum_{i=1}^n \theta_i \geq \frac{tm}{R} \right\} \\ &\leq \exp \left( -m \left( \frac{t}{R} \log \frac{t}{R} - \frac{t}{R} + 1 \right) \right). \end{aligned}$$

#### D. Epilogue

Using a different line of analysis in the vein of Rudelson and Vershynin (2008) and Dirksen (2015, Ch. 4), one may proceed under the  $\alpha$ -coherence assumption to obtain another set of results that establish restricted isometry for generative compressed sensing with subsampled isometries, as well as sample complexity and recovery bounds. Specifically, this line of analysis proceeds via generic chaining and a careful application of Dudley’s inequality, still leveraging the idea of  $\alpha$ -coherence. Though this avenue permits one to weaken the notion of coherence slightly, its proof is significantly more involved and yields results that are essentially equivalent to the current work’s up to constants. In particular, we conjecture that moving beyond the  $k^2$  “bottleneck” that we have commented on above (see Conclusion) is likely to require tools beyond the notion of  $\alpha$ -coherence.